SCIENTIFIC REPORTS

OPEN

SUBJECT AREAS:
BIOMEDICAL ENGINEERING
REPRODUCTIVE TECHNIQUES
EXTRACELLULAR SIGNALLING MOLECULES
HEART FAILURE

Received
13 May 2013

Accepted
20 December 2013

Published
16 January 2014

Correspondence and requests for materials should be addressed to C.Y.W. (wangchy@bmi.ac.cn) or M.X. (xing@cc.umanitoba.ca)

* These authors contributed equally to this work.

Engineering the heart: Evaluation of conductive nanomaterials for improving implant integration and cardiac function

Jin Zhou[1]*, Jun Chen[2]*, Hongyu Sun[1]*, Xiaozhong Qiu[3]*, Yongchao Mou[1], Zhiqiang Liu[1], Yuwei Zhao[1], Xia Li[1], Yao Han[1], Cuimi Duan[1], Rongyu Tang[1], Chunlan Wang[1], Wen Zhong[4], Jie Liu[5], Ying Luo[5], Malcolm (Mengqiu) Xing[2] & Changyong Wang[1]

[1]Department of Advanced Interdisciplinary Studies, Institute of Basic Medical Sciences and Tissue Engineering Research Center, 27 Taiping Rd, Academy of Military Medical Sciences, Beijing, China, [2]Department of Mechanical and Manufacturing Engineering, Faculty of Engineering, Department of Biochemistry and Medical Genetics, Faculty of Medicine, University of Manitoba and Manitoba Institute of Child Health, Winnipeg, Manitoba, Canada, [3]Department of Anatomy, Southern Medical University, Guangzhou Guangdong, China, [4]Department of Textile Sciences, Faculty of Human Ecology, Department of Medical Microbiology, Faculty of Medicine, University of Manitoba, Canada, [5]Department of Biomedical Engineering, College of Engineering, 5 Yiheyuan Rd, Peking University, HaidianDist, Beijing, China.

Recently, carbon nanotubes together with other types of conductive materials have been used to enhance the viability and function of cardiomyocytes *in vitro*. Here we demonstrated a paradigm to construct ECTs for cardiac repair using conductive nanomaterials. Single walled carbon nanotubes (SWNTs) were incorporated into gelatin hydrogel scaffolds to construct three-dimensional ECTs. We found that SWNTs could provide cellular microenvironment *in vitro* favorable for cardiac contraction and the expression of electrochemical associated proteins. Upon implantation into the infarct hearts in rats, ECTs structurally integrated with the host myocardium, with different types of cells observed to mutually invade into implants and host tissues. The functional measurements showed that SWNTs were essential to improve the performance of ECTs in inhibiting pathological deterioration of myocardium. This work suggested that conductive nanomaterials hold therapeutic potential in engineering cardiac tissues to repair myocardial infarction.

Engineering cardiac tissues *in vitro* offers new perspectives for the therapy of myocardial infarction (MI)[1–9]. The Engineered cardiac tissues (ECTs) exert beneficial effects on heart function after implantation, however, the therapeutic efficacy in general is restricted to inhibit further pathological deterioration of infarct myocardium without expected complete reversal of myocardial dysfunction[3,4,8,9].

A prerequisite for successful myocardial repair is that the implanted ECTs can electrically couple with host tissue and participate in the synchronous contraction of the whole heart[10,11]. Although the ECTs closely attached to the surface of host myocardium after implantation, there was still a clear boundary between ECTs and host tissues within the infarct areas due to the inadequate structural integration between ECTs and infarct myocardium[1,8]. Since the structural integration of ECTs into infarct areas was insufficient, the capacity of ECTs to regulate the microenvironment of infarct areas could not be fully developed, which hampered the therapeutic efficacy of ECTs for the myocardium infarction[1–3,8].

The biomaterial scaffold is the main component of engineered cardiac tissues[12]. Currently, biomaterials that have been used for fabricating ECTs scaffolds range from synthetic polymers[7,13,14], to naturally derived matrixes[5,6,15] and to biologically inspired materials[16]. In previous studies, it has been proved that the biomaterial scaffolds can promote cardiac cells to form three dimensional ECTs with native structural and contractile properties *in vitro*[15,17–19], support ECTs attachment and survival in the infarcted myocardium after implantation, and exert beneficial effects on improving heart function[5,6,8,13].

Nevertheless, the conventional materials showed a certain limitation in aspect of improving the effect of structural and functional integration between ECTs and infarct myocardium. Considering the structural and electrical conductive property of native myocardium[20,21], conductive nanomaterials that can provide solutions in this regard have been used to hybridize with natural materials to construct ECTs with stronger contractile and electrical properties[22–24]. Despite all these efforts, it is noted that the application of conductive nanomaterials only

restricts to constructing ECTs *in vitro*, and it remains to be elucidated whether conductive nanomaterials can support functional ECTs formation *in vivo*, or exert beneficial effects on the heart function, or support the structural and functional integration between ECTs and infarcted myocardium based on their nanoscale properties.

Carbon nanotubes are at the forefront of nanotechnology due to their unique electrical and mechanical properties[25–28]. It has been demonstrated that carbon nanotubes can improve the viability and proliferation of cardiomyocytes and promote their electrophysiological maturation[29–32]. Carbon nanotubes modified with natural or synthetic polymers have allowed for a variety of biological applications such as biochemical sensing, drug delivery, as well as tissue engineering[33–35]. Given that gelatin is a kind of biocompatible materials derived from extracellular matrix, it has been reported that carbon nanotubes-incorporated gelatin methacrylate (CNT-GelMA) hydrogel thin film can be used to engineer 2D cardiac patches[32]. Nevertheless, it remains to be elucidated that whether cardiac patches based on CNT composites can exert beneficial effects on the heart function after myocardial infarction.

In this study, we hypothesized that: 1) SWNT/gelatin composite scaffolds can be used to fabricate ECTs with strong contractile and electrical properties, promote the repair efficacy of ECTs to infarct myocardium, and enhance the integration between ECTs and host myocardium; 2) the SWNTs can migrate into infarct areas due to their unique nanoscale properties, and SWNTs can regulate the microenvironment of infarct myocardium to enhance the structural integration, even the fusion of ECTs into the infracted myocardium.

Results

Preparation of SWNT/gelatin hydrogels. SWNT/gelatin hydrogels were fabricated by mixing SWNTs with gelatin, followed by glutaraldehyde (GA) cross-linking. To obtain uniform carbon nanotubes dispersion, different solvents were tested and trifluoroethanol was found to give rise to hydrogels with fast gelling speed and homogeneous structures, as compared to water, PBS buffer, ethanol/methonal and acidic solution. The gross morphology of SWNT/gelatin hydrogels and gelatin hydrogels was showed in supplementary Fig. S1.

To determine the optimal concentration of SWNTs, we systematically evaluated the cytotoxicity of SWNT/gelatin composite scaffolds with different SWNTs concentration (0, 0.5, 1, 1.5, 2 and 2.5 mg/mL) on cardiac cells based on the previous reports[36–38]. Viability/Cytotoxicity assay showed that the cytotoxicity of SWNT/gelatin composite scaffolds on cardiac cells was closed related to the concentration of SWNTs (supplementary Fig. S2). The cardiac cell viability was maintained in a stable level of more than 80% after 3 days' culture when the concentration of SWNTs was less than 2 mg/mL, however it dramatically deceased from $87.3\pm3.4\%$ to 68.1 ± 3.6 when the concentration of SWNTs increased from 1.5 mg/mL to 2 mg/mL respectively. Considering that the electrical and mechanical properties of carbon nanotubes also depend on their concentration[30–32], we chose 1.5 mg/mL SWNTs to be incorporated with 7.5% gelatin and 2.5% GA to fabricate the composite hydrogels.

Scanning electron microscopy (SEM) observation of SWNT/gelatin showed that the scaffolds possessed a highly microporous structure and a well-developed network in which coil SWNTs were uniformly distributed (Fig. 1a). The surface of pore walls appeared smooth without adherence of aggregated SWNTs. At high magnifications, it was observed that tubular structure of SWNTs ending on the surface of the pore walls. Generally, SWNT/gelatin hydrogels exhibited significantly higher mechanical stress in comparison with the pure gelatin scaffolds under the condition of 7.5% gelatin (Fig. 1b). However, this trend reversed when the concentration of gelatin increased to 15%, which may be duo to the accumulation of SWNTs with the decrease in the porosity and pore size of gelatin. Besides, the conductivity of SWNT/gelatin hydrogels (containing 1.5 mg/mL SWNTs, 7.5% gelatin and 2.5% GA) was found to be significantly greater compared with gelatin hydrogels (Fig. 1c).

Construction and evaluation of ECTs *in vitro*. To determine whether SWNT/gelatin hydrogels are appropriate for constructing ECTs, neonatal rat cardiac cells were seeded into SWNT/gelatin scaffolds to construct carbon nanotubed ECTs (c-ECTs). The ECTs constructed without SWNTs were designated as g-ECT. All groups were cultured under static conditions for 3 days, following 5 days' electrical field stimulation as previously reported[29] to enhance their electrical performance. Three dimensional (3D) live cell imaging of c-ECTs showed the process of cell proliferation and migration into SWNT/gelatin scaffolds and the organization of cardiac tissues (Fig. 2a, Supplement Movie M1,). With time, the multi-cellular aggregates within SWNT/gelatin scaffolds became more compact upon electrical field stimulation compared with the constant small sporadic aggregates in gelatin scaffolds (Fig. 2b). Besides, we tested cell types and their proportion in c-ECTs groups at day 3 and day 8 by immunofluorescence analysis. It demonstrated that the percentages of cardiomyocytes, fibroblasts, vascular smooth muscle cell and endothelial cells was 63.6%, 24.5%, 8.9% and 2.8% at day 3, while they changed to 48.3%, 34.8%, 14.4% and 3.3% at day 8, respectively (Supplementary Fig. S3).

To further assess the effects of carbon nanotubes on the function of cardiac cells, the expression of cardiac troponin T (cTnT)/sarcomeric actinin and connexin (Cx43) in c-ECTs were analyzed in order to understand the myofilament reassembly and gap junction formation respectively. Abundant cTnT-positive cardiomyocytes were observed, as well as organized dense aggregates in c-ECTs (Fig. 2d). Meanwhile, cardiomyocytes also exhibited strong expression of Cx43 (the main protein of gap junctions) along the cell plasmalemma and between adjacent cells, such phenomenon was not observed in the g-ECT groups (Fig. 2d). Western blotting further revealed that c-ECTs had a statistically-significant increase in Cx43 and actinin expression compared with g-ECTs groups ($p<0.01$, Fig. 2e, and Supplementary Fig. S4–b).

Meanwhile, to better clarify the effect of electrical field stimulation, non-stimulated controls of c-ECTs and g-ECTs were tested by immunofluorescence and western blotting assay. It was demonstrated that electrical field stimulation could upregulate the expression of actinin both in c-ECT and g-ECT groups. Furthermore, electrical field stimulation could promote the polarization of Cx43 in c-ECT groups which play an important role in the coordination of electrical currents (Supplementary Fig. S5).

To assess the maturation of cardiomyocytes, we investigated the ultra-microstructure of c-ECTs under transmission electron microscopy (TEM) (Fig. 2c). It is noted that most of the cardiomyocytes were densely packed with myofibrils and displayed a predominant orientation of sarcomere composed of Z bands along the longitudinal cell axis, while the cardiomyocytes showed progressively less organized sarcomeres within gelatin scaffold (Fig. 2c). Intercalated discs, specialized cell-cell junctions that were responsible for mechanical and electrical coupling of myocardium, formed between adjacent cardiomyocytes. SWNTs were observed to disperse in the interspaces between cardiomyocytes and in direct contact with the cardiac cell membranes. After 21 days of culture, the distribution of SWNTs on cardiac membrane was extended and accompanied with adjacent membranes concavity and vesicles. In terms of the enhanced myofilament reassembly and gap junction formation in c-ECTs, it may rely on the direct interaction between SWNTs and cardiomyocytes which might induce specific change in membrane electrical behavior[36].

To compare the contractile and electrophysiological performance of c-ECTs with g-ECTs, we imaged them by calcium-sensitive dye and recorded the green fluorescence intensity of five separate sites (Fig. 2f). We noticed that g-ECTs did not contract visually after 8 days' culture and showed little spontaneous electrical activity under

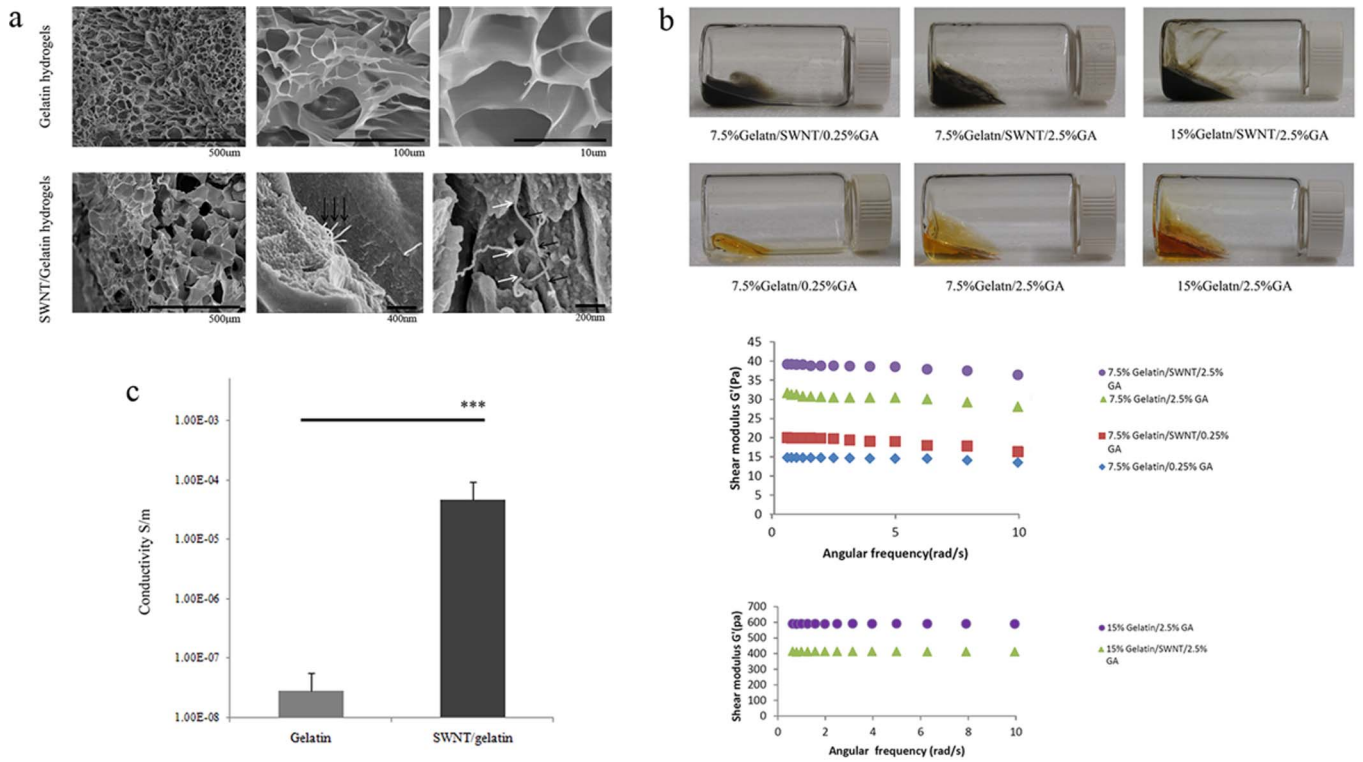

Figure 1 | Preparation and evaluation of SWNT/gelatin hydrogels. (a), SEM images showed the highly microporous structure of gelatin hydrogels and SWNT/gelatin hydrogels. Carbon nanotubes were well dispersed in gelatin hydrogels (G) with the appearance of networks connecting the pore of gelatin hydrogels. High magnifications revealed the tubular structure (black arrows) of carbon nanotubes ending (white arrows) on the surface of the pore walls. (b), Representative macro images from each group of gelatin hydrogels and SWNT/gelatin hydrogels with different concentration of gelatin and GA. The SWNT incorporation into the gelatin hydrogels enhanced their mechanical stress compared to the pure gelatin scaffolds were observed under the condition of 7.5% gelatin while this trend reversed when the concentration of gelatin increased to 15%. (c), The conductivity of SWNT/gelatin hydrogels (containing 1.5 mg/mL SWNTs, 7.5% gelatin and 2.5% GA) was found to be significantly greater compared with gelatin hydrogels. *** denotes statistical significance for the conductivity of SWNT/gelatin hydrogels compared to gelatin hydrogels, $P<0.001$, error bars, ±s.d.

calcium image. In contrast, c-ECTs beat regionally after 2–3 days and contracted synchronously at day 8 (Supplementary Movie M2). The c-ECTs displayed apparent spontaneous electrical activity at each site and calcium transients with partial synchronism (Supplementary Movie M3). After point stimulation under calcium imaging, four tested sites (No.1 to No.4) in c-ECTs showed complete synchronism activity from stimulated sites within 300 μm, while the fifth site about 360 μm away from stimulated sites showed partial synchronism activity (Supplementary Movie M4). It suggested that the synchronously electrical propagation was about 300 μm in c-ECTs.

Implantation and integration of ECTs with host. For *in vivo* application, c-ECTs were implanted into Sprague-Dawley (SD) rats with large myocardial infarct, and g-ECTs, composite hydrogels with non-cardiomyocytes (NCM) grafts, and sham were performed as controls. Operations were performed at 14d after left anterior descendant coronary (LAD) ligation, rats with heart fractional shortening (FS)<30% were selected (Supplementary Table T1). CM-DiI (2 μmg/mL) was used to label cells in ECTs before implantation to track implanted cells.

1 week after engraftment, c-ECTs attached to the infarct region of host myocardium. Most of cell aggregates distributed within the pores of SWNT/gelatin hydrogels with vessel-like structures located inside, while better-aligned cell bundles appeared at the edge of scaffolds (Fig. 3a). Immunostaining showed c-ECTs-derived DiI^+ cardiomyocytes developed a differentiated phenotype with abundant expression of Cx43 (Fig. 3b). Besides, DiI^+ implanted cardiomyocytes and SWNTs located within c-ECTs and few could be detected in the host myocardium and scar areas after 1 week of engraftment. $DiI^- + vWF^+$ (von Willebrand factor) blood vessels were detected in c-ECTs, suggesting that host's vasculature has invaded into the c-ECTs at early stage.

Four weeks following engraftment, c-ECTs were still observable in the infarct regions generally with unclear boundary to infarct myocardium (Fig. 3c, Supplementary Fig. S6). Along with the partial degradation of gelatin hydrogels, some SWNTs emerged outside the gelatin scaffolds and incorporated to form well-aligned cell bundles, while the number of blood vessels with erythrocytes increased obviously (Fig. 3c, 3d). In c-ECTs, DiI^+ implanted cardiomyocytes developed and expressed Cx43 for electrical integration (Fig. 3d). Notably, DiI^+ cardiomyocytes migrated from c-ECTs into the scar areas, accompanied by the transportation of SWNTs into the scar areas, suggesting that c-ECTs structurally integrated to the host myocardium through cell and scaffolds migration (Fig. 3c, 3d).

Besides, four types of DiI^- cells emerged in c-ECTs (Fig. 3d): 1) cTnT positive cardiomyocyte; 2) SMA (α-smooth muscle actin) positive smooth muscle cells (which formed blood vessels connecting to the host's vasculature); 3) PCNA (proliferating cell nuclear antigen) positive proliferating cells; 4) CD68 positive macrophages. Some of the DiI^- cells in c-ECTs might come from the host, suggesting that the host also integrated to the engraftment structurally. The phenomenon that various host cells migrated into the c-ECTs further demonstrated that apparent structural integration occurred between ECTs and host myocardium.

Integration of c-ECTs to host myocardium through SWNTs migration. To further explore the contribution of the environment within host myocardium to SWNTs migration, we compared the

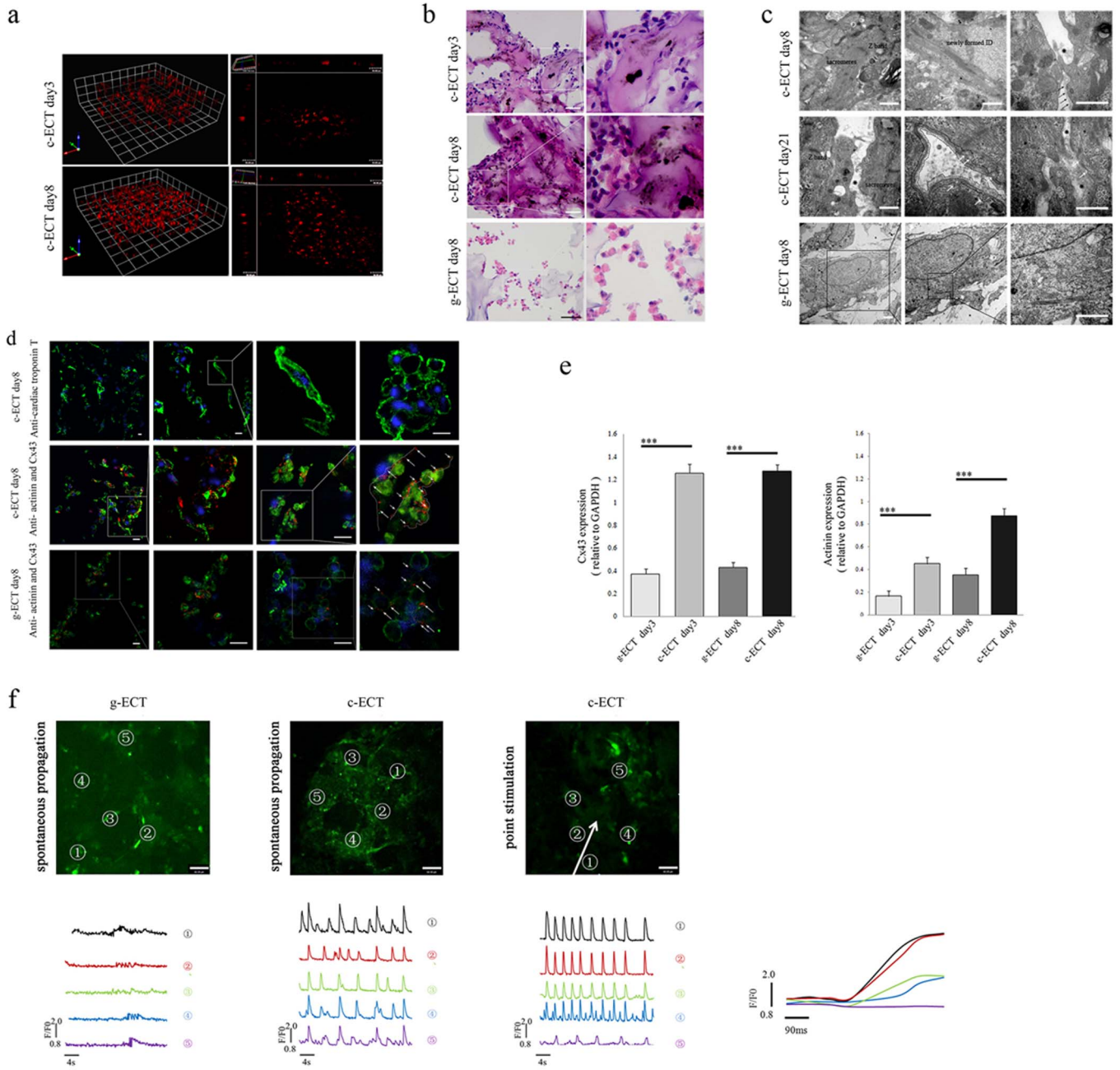

Figure 2 | Construction and evaluation of c-ECTs. (a), 3D live cell imaging showed the process of cell proliferation and migration into SWNT/gelatin hydrogels to organize cardiac tissues from day3 to day8. (b), H&E staining of the c-ECTs on day 3 and day 8 revealed a better organized and more compact multi-cellular aggregates within the SWNT/gelatin scaffolds after electrical field stimulation, however, g-ECTs on day 8 remained the constant small sporadic aggregates. (c), TEM showed the ultra-microstructure of c-ECTs at day 8 with apparent oriented sarcomeres, Z bands, newly formed intercalated disc, and directly contact of carbon nanotubes at localized sites of cardiac membrane surface (black arrow), while the cardiomyocytes showed progressively less organized sarcomeres within the gelatin scaffold. After culture for 21 days, the distribution of carbon nanotubes on cardiac membrane became continuous (within black dotted line) with adjacent membranes concavity (white arrow) and vesicles formation (white dotted line). (d), Immunostaining of c-ECTs on day 8 revealed pervasive cTnT expression (green) and Cx43 gap junction protein (red, white arrow and dotted line) were found between sarcomeric actinin positive cardiomyocytes (green) compared with low expressions in g-ECTs. Nuclei were stained blue. (e), Quantification of sarcomeric actinin protein and Cx43 protein expression by western blot. (f), Calcium transient was assessed at specified 5 points by monitoring calcium dye fluorescence (green). c-ECTs displayed apparent spontaneous electrical activity at each sites compared with little spontaneous electrical activity in g-ECTs. After point stimulation, four tested sites (No.1 to No.4) in c-ECTs showed complete synchronism activity from stimulated sites within 300 μm. The white arrow represents the direction of propagation. F/F_0 refers to measured fluorescence normalized to background fluorescence. Scar bars, 100 μm (b), 20 μm (d) or 60 μm (f).

regularity of SWNTs migration in infarct heart with that in healthy heart (as control) after 4 weeks of implantation. We noticed that some SWNTs migrated into the scar areas of infarct heart (Figure 4a). They located at intercellular space, as well as on cell membrane surface or in cytoplasm. In the infarct area, cells preferred to adjoining SWNTs to form dense cell bundles or clusters, thus SWNTs could connect cells continuously at local sites in the scar area, even throughout the infarct area (Figure 4b).

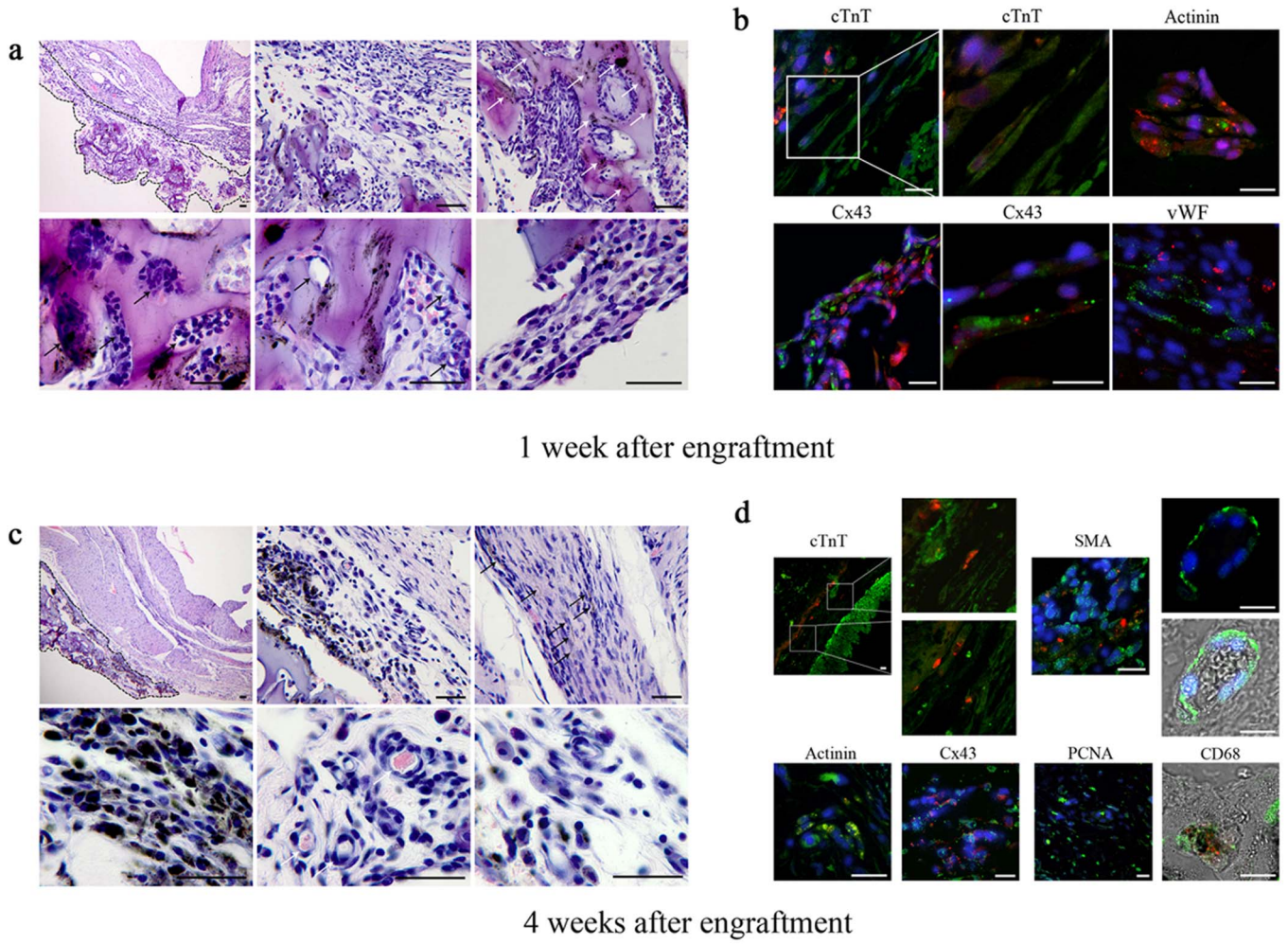

Figure 3 | Morphology of c-ECTs after engraftment into infarct myocardium. (a), H&E staining of the mid-ventricular 1 week after engraftment showed that c-ECTs firmly attached to the infarct surface (black dotted line). Most carbon nanotubes distributed within gelatin hydrogels (white arrow). Tissue aggregates distributed within the pore and showed vessel-like structures (black arrow), while better-aligned cell bundles appeared at the edge of scaffolds. (b), Immunostaining showed c-ECTs-derived DiI^+ cardiomyocytes (green+ red) developed a differentiated phenotype with abundant expression of Cx43 (green+ red). vWF positive blood vessels (green) appeared within c-ECTs. (c), H&E staining of the mid-ventricular 4 weeks after engraftment showed the morphology of c-ECTs attached to the infarct surface (black dotted line). Carbon nanotubes dispersed throughout the c-ECTs and migrated into the scar area (black arrow). Blood vessels with erythrocytes formed obviously (white arrow). (d), Immunostaining showed DiI^+ cardiomyocytes migrated into the scar areas (green+ red), while DiI^- cardiomyocytes appeared in c-ECTs (green). In c-ECTs, DiI^+ cardiomyocytes expressing actinin (green+ red) and Cx43 (green+ red) could be detected. Besides, some DiI^- cells (green) including SMA positive blood vessels with erythrocytes, PCNA positive proliferating cells and CD68 positive macrophages could also be detected. Nuclei were stained blue. Scar bars, 100 μm (a, c) or 20 μm (b, d).

As a control, when c- ECTs were implanted to healthy heart, SWNTs were mostly confined to c-ECTs and few could be detected in native myocardium (Figure 4c).

Besides, we further detected the distribution of macrophages. It could be observed that CD68 positive macrophages accumulated in the scar areas of myocardium and the fusional zone between c-ECTs and host myocardium (Fig. 4d, Supplementary Fig. S7). The amount of macrophages within the scar areas in c-ECT group was higher than in g-ECTs, non-cardiomyocytes (NCM) and sham groups (Fig. 4f, Supplementary Fig. S8). In particular, some of these macrophages in infarct areas contained phagotrophic SWNTs within their cytoplasm, suggesting that the migration of macrophages might play a role in the transportation of SWNTs. Also, we compared the location of macrophages when c-ECTs were implanted to healthy heart. It demonstrated that most CD68 positive macrophages were confined to c-ECTs as well as SWNTs (Figure 4e), which might be due to the native structure and property of normal heart without inflammatory microenvironment.

Functional consequence of ECTs integration. Four weeks after graft implantation, heart function was measured and compared between c-ECT group and control groups (g-ECTs, non-cardiomyocytes (NCM) and sham groups). In total, 102 rats survived after LAD ligation, while 73 rats had a fractional shortening (FS)$<$30% and 54 rats survived the complete study and were subjected to echocardiography analysis. Echocardiography showed that transplantation of c-ECTs significantly increased the FS and EF (ejection fraction), deceased LVESD (left ventricular end-systole dimension), and inhibited the progress of left ventricle enlargement compared with control groups, suggesting that the implantation of c-ECTs effectively inhibited further pathological deterioration and improved heart function. (Fig. 5a, Supplementary Table T2). Catheterization analysis provided consistent evidence with echocardiography analysis, that c-ECTs significantly enhanced diastolic and systolic function, including the increased left ventricle max dP/dt (change in pressure/change in time) and the decreased LVEDP (left ventricular end-diastolic pressure) (Fig. 5c, Supplementary Table T3).

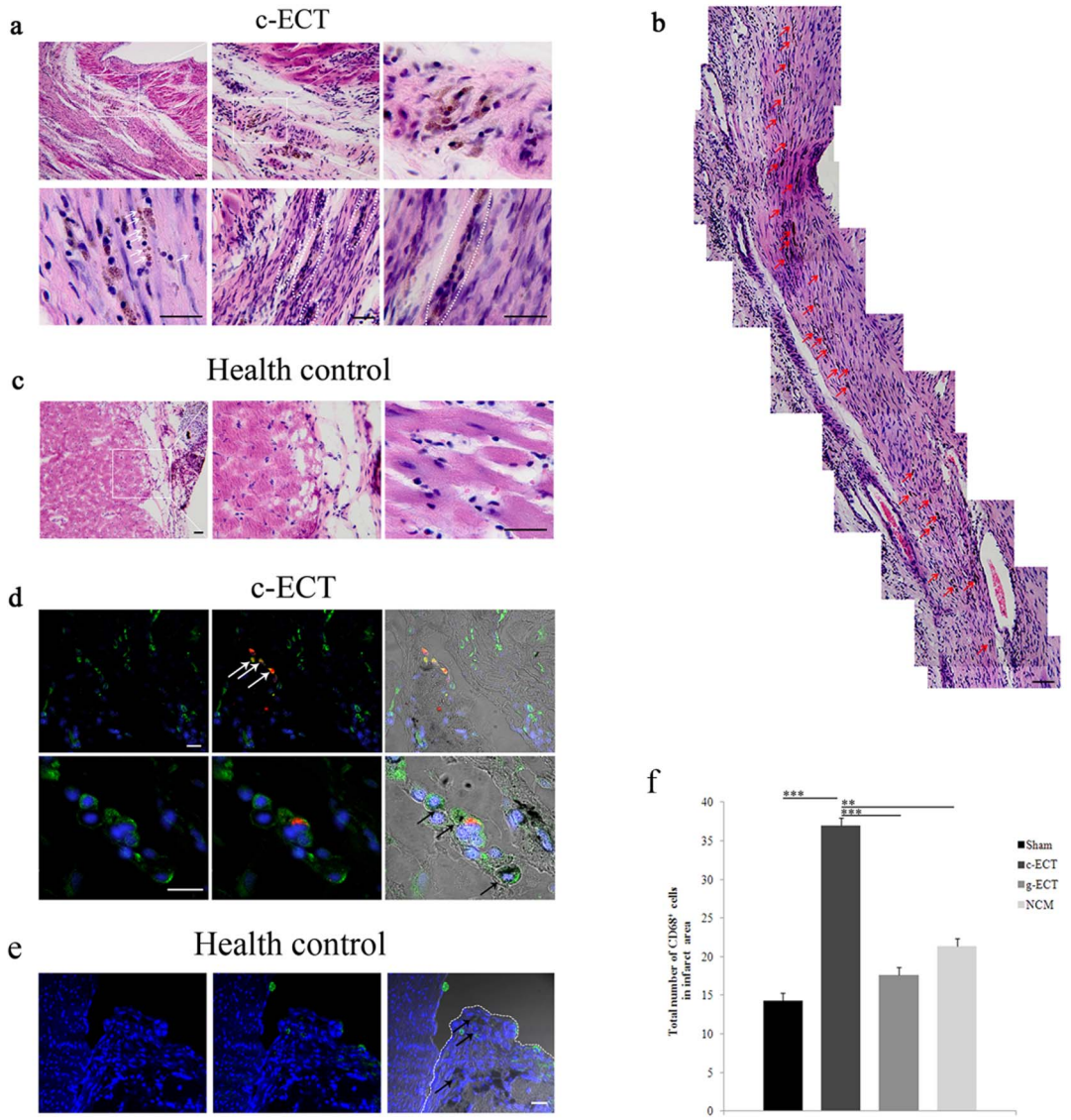

Figure 4 | Integration of c-ECTs to host myocardium through Carbon nanotubes migration. (a), H&E staining of the mid-ventricular 4 week after engraftment showed that carbon nanotubes migrated into the scar areas and located at cell membrane surface or in cytoplasm, as well as intercellular space(white arrow). Carbon nanotubes could connect cells to form dense cell bundle or clusters in the infarct area (white dotted line), even throughout the infarct area (b). Red arrows in (b) showed carbon nanotubes with continuous distribution. (c), Carbon nanotubes were mainly confined to the implants on the surface healthy heart as control. (d), Immunostaining showed CD68 positive macrophages (green) migrated from the c-ECTs to the infarct area, with apparent accumulation in the boundary zone and in scar areas. Some of these macrophages contained phagotrophic carbon nanotubes within their cytoplasm (black arrow), and some of them were c-ECTs-derived DiI^{+} macrophages (red+ green, white arrow). (e), CD68 positive macrophages (black arrow) were confined to the c-ECTs (white dotted line) on the surface healthy heart as control. Some of these macrophages contained phagotrophic carbon nanotubes within their cytoplasm (black arrow). (f), The number of CD68 positive cells in the infarct areas of c-ECTs compared with g-ECTs, NCM and sham groups. Nuclei are stained blue. Scar bars, 100 μm (a–c) or 20 μm (d, e). Data are mean ± s.e.m. *=$p<0.05$, **=$p<0.01$, ***=$p<0.001$.

Notably, c-ECTs grafting resulted in effective improvement of heart function compared with the other control groups (Fig. 5b, 5c), suggesting that c-ECTs based on SWNT provide significant therapeutic efficacy in repairing the infarct myocardium and functional integration with the host heart.

Molecular mechanism underlying the effects of SWNTs on cardiac repair. To further understand the potential role of carbon nanotubes in the process of heart repair by c-ECTs, we investigated the expression of intercellular adhesive junctions and electrochemical junctions, as well as their relevant molecular pathways. Western blot analysis revealed stronger upregulation of N-cadherin and Cx43, a modest increase of Nav1.5 in the c-ECTs-treated rats compared with that in g-ECTs, NCM and sham groups (Fig. 6a, 6b), implying that the addition of SWNTS enhanced the expression of intercellular adhesive junctions and electrochemical junctions in the c-ECTs-treated rats. Given that the integrity of intercellular adhesive junctions is a prerequisite for electrochemical junctions formation, we assessed the integrin-mediated mechanotransduction pathway, including the target molecules ILK (integrin-linked kinase), AKT (also known as Protein kinase B) and ß-catenin. We found that ß1-integrin levels were higher in c-ECTs groups compared with that in g-ECTs, NCM and sham groups. Especially, ILK levels and p-AKT levels in c-ECTs were significantly higher (Fig. 6c, 6d). Similar results were observed for ß-catenin levels, which also can be regulated by ILK. The activation of ILK, p-AKT and ß-catenin in the

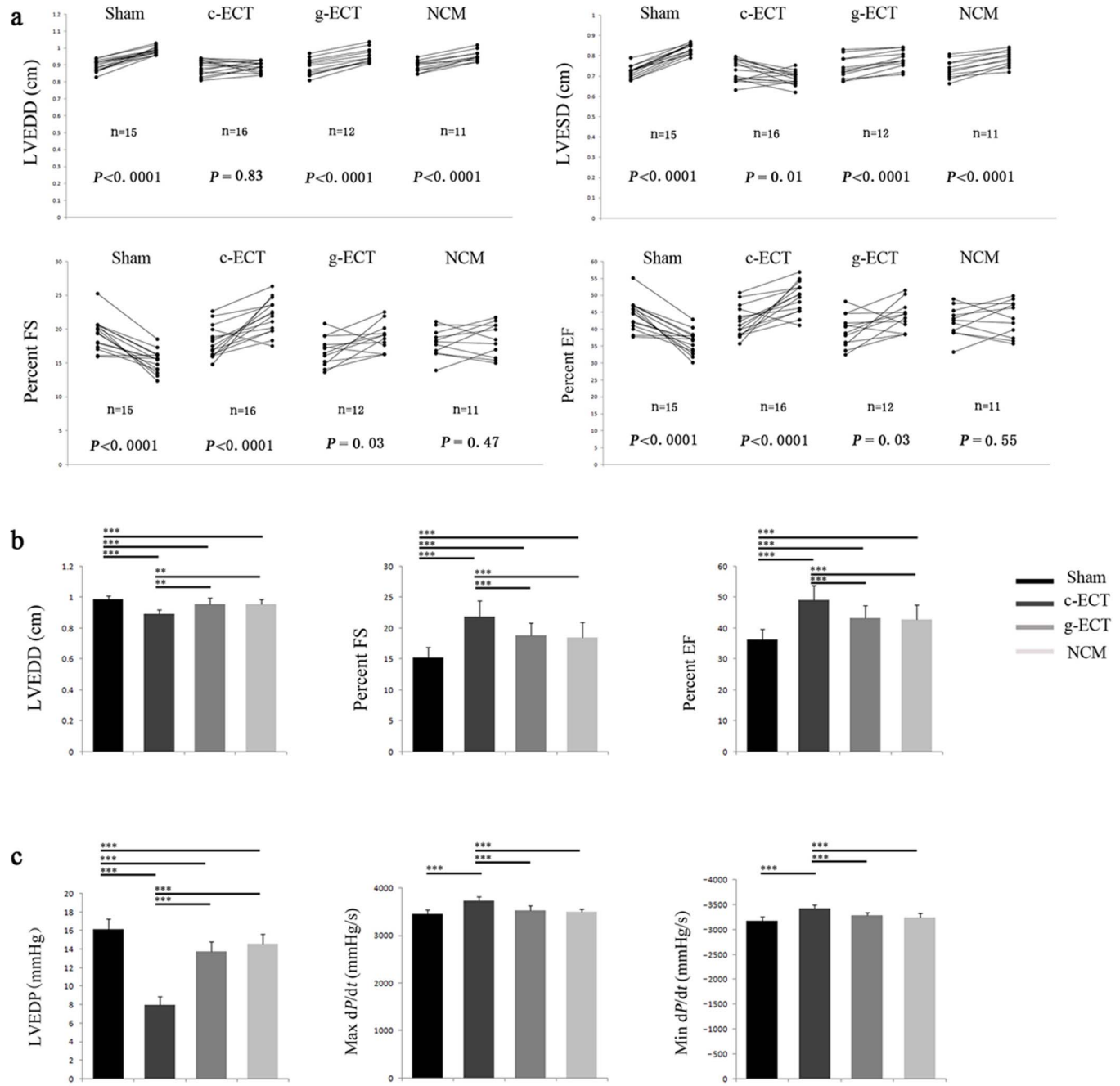

Figure 5 | Changes in left ventricular function after implantation for 4 weeks. (a), Each rat survived was reevaluated after implantation for 4 weeks. Trajectories showed the change of LVEDD, LVESD, FS and EF for each rat determined by echocardiography pre-implantation and after-implantation. Statistical evaluations were performed by paired two-tailed Student *t*-tests. (b), Comparison of left ventricular function determined by echocardiography (LVEDD, FS and EF) between each groups after 4 weeks of implantation. (c), Comparison of left ventricular function determined by catheterization(LVEDP, Max d*P*/d*t* and Min d*P*/d*t*) between each groups after 4 weeks of implantation. Data are mean ± s.e.m. *=$p<0.05$, **=$p<0.01$, ***=$p<0.001$. Abbreviations: LVEDP, left ventricular end-diastolic pressure; d*P*/d*t*, change in pressure/change in time; LVEDD, left ventricular end-diastolic dimension; LVESD, left ventricular end-systole dimension; FS, fractional shortening; EF, ejection fraction; NCM, non-cardiomyocytes grafts.

infarcted region of c-ECT-treated rats suggested that ILK/Akt/ß-catenin pathway might involve the beneficial effect of SWNTs on cardiac repair.

Discussion

We demonstrated the hypothesis that ECTs constructed by SWNT/gelatin composite scaffolds could effectively repair the infarct myocardium through the nanoelectronic conductive scaffolds mediated integration. Our data showed that ECTs based on SWNT/gelatin composite scaffolds showed stronger contractile and electrical properties *in vitro*. After implantation, ECTs could integrate to infarct myocardium and exerted beneficial effects on the myocardial regeneration and remodeling in the infarct areas, resulting in the improvement of heart function. We believe that our study can serve as a proof of principle for a therapeutic potential of nanoelectronic conductive scaffolds in myocardial repair.

In previous studies, efforts have been made to improve the muscle-mimicry property of scaffolds in terms of chemistry, mechanics and microstructure[13,19,22–24]. One key functional trait of the native myocardium is the excitation-contraction coupling which converts the

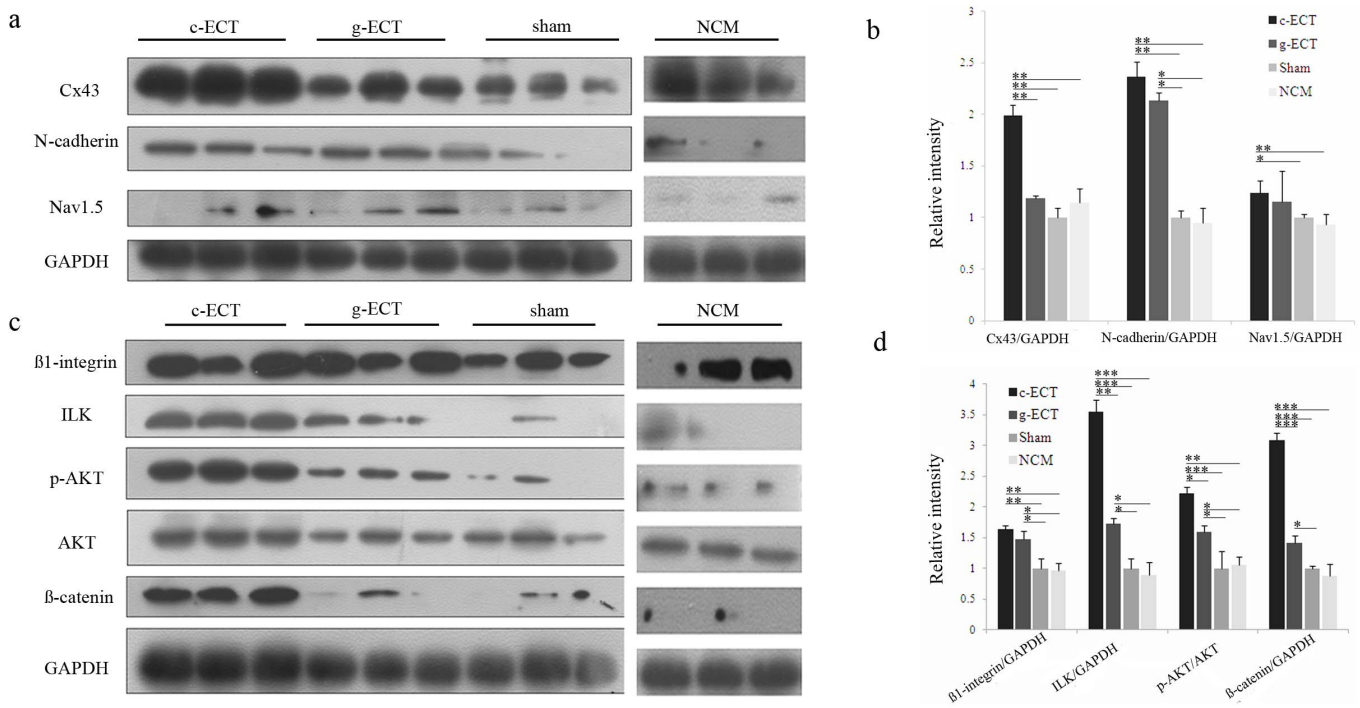

Figure 6 | Molecular mechanism underlying the beneficial effect of SWNT on cardiac repair. (a), Western blot analysis of the expression of Cx43, N-cadherin, Nav1.5 in the ischemic zones lysates after implantation for 4 weeks. (c), Western blot analysis of the expression of integrin-mediated ILK signaling molecule in the ischemic zones lysates after implantation for 4 weeks. The antibodies against ß1-integrin, ILK, Akt phospho-Akt (Ser473) and ß-catenin were used. (b, d), Bar graphs showing quantification of the expression level of each protein compared with the expression of GAPDH or the non-phosphorylated isoform. Lanes 1–3 show data from individual rats of the c-ECT group; lanes 4–6 show data from individual rats of the g-ECT group; lanes 6–9 show data from individual rats of the sham group; lanes 10–12 show data from individual rats of the NCM group. Data are mean ± s.e.m. *=$p<0.05$, **=$p<0.01$, ***=$p<0.001$.

action potential of the cell membrane into muscular contraction[20,21]. However, it still needs to be improved in ECTs. Carbon nanotubes can provide solutions in this regard with their intriguing mechanical and electrical properties. Previous studies have shown that carbon nanotubes could promote cardiac cells adhesion, proliferation and maturation, and enhance cell-cell electrical coupling in 2D environments[29–32] indicating their potential to construct functional 3D ECTs *in vitro*. On the basis of 2D patches and 3D biohybrid actuators constructed by CNT hydrogel sheets by Ali K. group[31], we further engineered the 3D patches with a certain thickness using the CNT based hydrogel *in vitro.* Our study serves as a proof of principle to further demonstrate that conductive nanomaterials (SWNTs) not only supported the contractile property of ECTs, but also enhanced the formation of gap junction and promoted the excitation-contraction coupling of cardiomyocytes in ECTs through direct contacts with cardiomyocytes. It would possess appropriate electrical compatibility between ECT cells and host tissues to allow coordinated excitation of ECTs and their integration with impaired myocardium.

In the past years, conductive nanomaterials of carbon nanotubes emerged as promising candidate scaffolds in tissue engineering research. They have been wildly used to hybridize with natural materials to increase the mechanical and electrical properties of base polymers[30–32,34,39]. In order to improve the properties of carbon nanotube-composite scaffolds, careful consideration of carbon nanotubes dispersion is required to achieve the desired electrical conductivity and reduce the cytotoxicity, since the strong tendency of carbon nanotube to agglomerate could impair cell viability[40,41]. To obtain uniform carbon nanotubes dispersion, we tested different solvents and found that trifluoroethanol could lead to fast gelling speed and homogeneous structures, compared with water, PBS buffer, ethanol/methonal and acidic solution. Based on Viability/Cytotoxicity assay, we found that SWNT/gelatin had little cytotoxic effects on cardiac cells.

An important observation of this study is that the implanted c-ECTs structurally fused with the infarct myocardium and carbon nanotubes may play a vital role in this process. The phenomenon that transplanted cells migrated from c-ECTs into the infarct areas and carbon nanotubes were transported into the infarct myocardium, while host cells infiltrated into c-ECTs, suggesting the fusion of implanted c-ECTs with the infarct myocardium. In particular, the host vasculature invaded the graft 1 week after transplantation and increased significantly 4 weeks after transplantation, which could provide sufficient nutrition for the grafts and ensure vitality and function of the grafts *in vivo*[42,43]. Considering that the conductivity of heart would be reduced due to the infarct myocardium (resulting in unavailing impulse transmission and contraction[24]), the continuous distribution of SWNTs may be beneficial to motivate the electrical conduction through the infarct area. Besides, considering the advantage of carbon nanotubes in enhancing the adhesion and proliferation capacity of cardiomyocytes[29,30,32], the SWNTs in infarct areas may also enhance the activity and regeneration capacity of cardiomyocytes in these areas. Thus, the transportation of SWNTs into infarct regions played a significant role in regulating the microenvironment and stimulating the native cells to migrate into infarct areas, which would be beneficial to myocardial regeneration and remodeling.

Another important observation of this study is that macrophages emerged in the process of the integration of c-ECTs to the host myocardium. Four weeks after transplantation, we found that CD68 positive macrophages apparently accumulated in the scar areas of myocardium and the fusional zone between ECTs and host myocardium. For this analysis, the macrophages may have two sources: 1) host derived macrophages due to their inflammatory

microenvironment and the reaction to the implanted ECTs containing SWNTs; 2) donor derived macrophages in ECTs from primitive cultured cells in SWNT/gelatin scaffolds. We inferred that the implantation of SWNT/gelatin scaffolds may trigger the inflammatory response, which is consisting with the recent reports[3,43–46]. As for the role of macrophages in influencing myocardial repair, it has been reported that they may participate in the angiogenesis[46,47]. Nevertheless, their role in the structural integration between ECTs and infarct myocardium has not yet been well understood. Our research provides a cue to explore the potential role of macrophages in this process. The emerging cause and mechanism of the macrophages, as well as their role in the structural integration between ECTs and host tissues deserved in-depth investigation.

We reported for the first time that ECTs based on conductive nanomaterials could improve heart function after MI. Furthermore, our data showed that the implantation of ECTs structurally integrated with host myocardium, inhibited further pathological deterioration of infarct heart effectively. One possible explanation is that the implanted ECTs replaced the damaged myocardium and attenuated dilation of left ventricular through the close attachment to the surface of infarct myocardium physically. In addition, the effective improvement of heart function may result from the infiltration of SWNT and implanted cells into the infarct myocardium. The presence of SWNT and implanted cells in the infarct areas directly regulated the microenvironment, promoted the myocardial remodeling in infarct areas and enhanced the regenerative capacity of cardiomyocytes in these areas. Take together, the integration and fusion of ECTs to the infarct myocardium eventually resulted in the effective improvement of heart function.

The molecular mechanisms for beneficial effects of carbon nanotubes in cardiac repair are largely unclear. The ordered assembly of adhesive junctions and electrochemical junctions are essential to the function of cardiac tissues[48]. It has been reported that mechanotransduction signaling play key roles in the establishment of intercellular adhesive junctions between cardiomyocytes[49]. Considering the excellent mechanical and electrical properties of carbon nanotubes, it remains to be elucidated whether the special microenviroment formed by carbon nanotubes can trigger mechanotransduction signaling. In cell-matrix interaction-induced biomechanical signals, ILK has been shown to plays an important role in regulating cardiac contractility[50], survival, and repair[51]. Activated by cell–matrix or growth factor, ILK signaling would further trigger the downstream molecules, including Akt, glycogen synthase kinase (GSK)3ß, p38 mitogen-activated protein kinase (p38MAPK), extracellular signal-regulated kinases (ERKs) and mTOR[51]. The study demonstrated ILK and p-AKT and ß-catenin were activated in the infarct region of c-ECT-treated hearts, while inactivated in the infarct region of control ones, suggesting that carbon nanotubes might trigger the ILK/Akt/ß-catenin pathway which may involve in the cardiac repair. The exact molecular mechanisms deserved further investigations.

In previous study, engineered cardiac patches have been transplanted immediately[52], 3 h later[53], 1 week later[54], 2 weeks later[1], and 4 weeks later[55] after acute infarction. In this study we transplanted ECTs 14 days after LAD ligation based on two reasons: 1) Clinically, the patients' heart function is not stable immediately after acute MI, and interventional therapy by thrombolysis is preferred at this stage to recover the patients' coronary arteries flow. 10–14 days post-MI, the patients' heart function gradually stabilizes and it is more suitable to perform further treatment[56]. 2) Generally, inflammation is intense in infarct myocardium immediately after acute MI[57,58]. It is unfavorable for the implanted ECTs at this stage to survival and work. However, after 10–14 days, the inflammation is greatly attenuated. This clinical phenomenon is in accordance with that in rat models of MI.

In summary, we have constructed 3D ECTs with good structure, phenotype and function based on conductive SWNT incorporated hydrogel scaffolds *in vitro*. Furthermore, we demonstrated, for the first time, that ECTs based on conductive nanomaterials could improve heart function *in vivo*. Notably, ECTs appeared obvious structural fusion with the infarct myocardium after implantation, which enhanced the remodeling and regeneration of the infarct myocardium. Despite the unresolved questions, our study provides a promising therapeutic perspective of conductive nanomaterials in cardiac tissue engineering/regeneration.

Methods

Preparation of SWNT/gelatin scaffolds. All chemicals were purchased from Sigma-Aldrich. SWNT were obtained from US Nanomaterials Research Inc. To disperse SWNT in Pluronic aqueous solution, the 10 mL of 2% Pluronic copolymer solution was prepared and 20 mg of SWNT were dispersed into the solution, and the mixture was ultra-sonicated for 1 min × 10 times, followed by centrifugation at 8000 rpm for 10 min, resulting in a homogeneously black solution. 30% of gelatin stock solution was prepared in 2, 2, 2-trifluoroethanol. Then quantitative amount of double distilled water (DDW) was added to make 7.5% of gelatin aqueous solution and the dispersed SWNT solution was added to make the final ratio at 2 wt% of gelatin, followed by the ultra-sonication for 1 min × 5 times with ice bath. A 25% glutaraldehyde solution (20 μL) was added to 180 μl of solution of SWNT/gelatin to give a final concentration of glutaraldehyde at 2.5%. The mixed solution was cast into a 24 well dishes, and then left at room temperature for 30 min to allow the cross-linking reaction of gelatin to proceed. 5% of sodium cyanoborohydride aqueous solution was added to immerse the hydrogels for 1 h to reduce the imine groups and to block the residual aldehyde groups of glutaraldehyde, followed by three times of DDW wash. The obtained hydrogels were immersed in DDW overnight for lyophilization. Regarding the preparation of gelatin scaffolds, we diluted 30% of gelatin stock solution into 7.5% gelatin and the cross-linking methods were same as above.

Engineering c-ECTs construction. Ventricular cardiac cells were isolated from 1-day-old neonatal Sprague-Dawley rats and seeded into SWNT/gelatin scaffolds to construct c-ECT (7×10^7 cells/cm^3). All c-ECTs were cultured under static conditions for 3 days, following 5 days' electrical field stimulation consistent to a previous report[22] to enhance their electrical performance. c-ECTs were transferred into a chamber fitted with two 1/4-inch-diameter carbon rods (Ladd Research Industries, Burlington, VT) placed 1 cm apart and connected to a cardiac stimulator (Nihon Kohden, Tokyo) with platinum wires (Ladd Research Industries). The cell constructs were cultivated in a cell incubator (37°C, 5% CO_2), under electrical stimulation (rectangular, 2 ms pulse, 5 V, 5 V/cm, 1 Hz).

Assessment of c-ECTs *in vitro*. The c-ECTs were assessed with the use of 3D live cell imaging, Live/Dead Viability/Cytotoxicity assay and histology staining to observe the cell attachment, viability, distribution, as well as the morphology of cardiac tissues in SWNT/gelatin scaffolds. In addition, immunohistochemical staining and western blotting were used to test the cardiac myofilament reassembly and gap junction formation in c-ECTs, which were also detected under TEM. Besides, we used intracellular calcium transient measurement to compare the contracted and electrophysiological performance of c-ECTs compared with g-ECTs as control. All details are available in the supplementary attachment of methods.

Myocardial infarction and c-ECTs grafting. All animal studies were approved by the Institutional Animal Care and Use Committee (IACUC) of the Chinese Academy of Military Medical Science (Beijing, China). Male Sprague-Dawley (SD) rats (300±2 g; n=136) were anesthetized with sodium pentobarbital (30 mg/kg) and were performed by permanent LAD ligation (6–0, Prolene, Ethicon). 14 days after generation of MI, the survived rats underwent an echocardiographic examination. The animals with FS < 30% by echocardiography were randomly divided into 4 treatment groups, which received the implantation of c-ECTs and g-ECTs, NCM grafts and sham operation. For the construction of g-ECTs and NCM grafts, neonatal rat cardiac cells and cardiac fibroblasts were seeded into gelatin hydrogel and the SWNT/gelatin hydrogel respectively. Grafts were simultaneously sutured onto the epicardial surface over the visible infarct myocardium and adjacent infarction border zones. In the sham-operated control group, 4 sutures were simultaneously performed as if ECTs were implanted. For immunosuppression, the animals were administered with daily injections of cyclosporine-A (5 mg/kg) azathioprine (2 mg/kg), and methylprednisolone (2 mg/kg) by subcutaneous injection. Prior to transplantation, all constructs were labeled with CM-DiI (Molecular Probes, Eugene, OR) for tracking the implanted cells in host myocardium.

Statistical analysis. The data distributions were checked for normality with the Shapiro-Wilk test and for equality of variances with the Levene procedure. An unpaired two-tailed Student *t*-tests was performed to compare 2 groups (*in vitro* data). We determined statistical differences using a paired two-tailed Student *t*-tests to evaluate echocardiography-determined left ventricular function after implantation compared to that of pre-implantation before. One-way analysis of variance (ANOVA) was used for multiple group comparisons of left ventricular function after 4 weeks' implantation. If the *F*-distribution was significant, we used the Newman-Keul procedure as a *post hoc* test. A P value of <0.05 was considered statistically

significant. Data were expressed as mean ± standard error of the mean (s.e.m.). All statistical analyses were performed in SAS statistical software version 9.1 (Cary, NC).

1. Zimmermann, W. H. *et al.* Engineered heart tissue grafts improve systolic and diastolic function in infarcted rat hearts. *Nat. Med.* **12**, 452–458 (2006).
2. Miyahara, Y. *et al.* Monolayered mesenchymal stem cells repair scarred myocardium after myocardial infarction. *Nat. Med.* **12**, 459–465 (2006).
3. Fujimoto, K. L. *et al.* An elastic, biodegradable cardiac patch induces contractile smooth muscle and improves cardiac remodeling and function in subacute myocardial infarction. *J. Am. Coll. Cardiol.* **49**, 2292–2300 (2007).
4. Landa, N. *et al.* Effect of injectable alginate implant on cardiac remodeling and function after recent and old infarcts in rat. *Circulation* **117**, 1388–1396 (2008).
5. Dvir, T. *et al.* Prevascularization of cardiac patch on the omentum improves its therapeutic outcome. *Proc. Natl Acad. Sci. USA* **106**, 14990–14995 (2009).
6. Tan, M. Y. *et al.* Repair of infarcted myocardium using mesenchymal stem cell seeded small intestinal submucosa in rabbits. *Biomaterials* **30**, 3234–3240 (2009).
7. Chen, Q. Z. *et al.* An elastomeric patch derived from poly(glycerol sebacate) for delivery of embryonic stem cells to the heart. *Biomaterials* **31**, 3885–3893 (2010).
8. Madden, L. R. *et al.* Proangiogenic scaffolds as functional templates for cardiac tissue engineering. *Proc. Natl Acad. Sci. USA* **107**, 15211–15216 (2010).
9. Jawad, H. *et al.* Myocardial tissue engineering: a review. *J. Tissue Eng. Regen. Med.* **1**, 327–342 (2007).
10. Furuta, A. *et al.* Pulsatile cardiac tissue grafts using a novel three-dimensional cell sheet manipulation technique functionally integrates with the host heart, in vivo. *Circ. Res.* **98**, 705–712 (2006).
11. Rubart, M. *et al.* Physiological coupling of donor and host cardiomyocytes after cellular transplantation. *Circ. Res.* **92**, 1217–1224 (2003).
12. Persidis, A. Tissue engineering. *Nat. Biotechnol.* **17**, 508–510 (1999).
13. Kim, D. H. *et al.* Nanoscale cues regulate the structure and function of macroscopic cardiac tissue constructs. *Proc. Natl Acad. Sci. USA* **107**, 565–570 (2010).
14. Zhang, Y. *et al.* The impact of PLGA scaffold orientation on in vitro cartilage regeneration. *Biomaterials* **33**, 2926–2935 (2012).
15. Ott, H. C. *et al.* Perfusion-decellularized matrix: using nature's platform to engineer a bioartificial heart. *Nat. Med.* **14**, 213–221 (2008).
16. Miyagi, Y. *et al.* Biodegradable collagen patch with covalently immobilized VEGF for myocardial repair. *Biomaterials* **32**, 1280–1290 (2011).
17. Zimmermann, W. H. *et al.* Cardiac grafting of engineered heart tissue in syngenic rats. *Circulation* **106**, I151–157 (2002).
18. Shimizu, T. *et al.* Fabrication of pulsatile cardiac tissue grafts using a novel 3-dimensional cell sheet manipulation technique and temperature-responsive cell culture surfaces. *Circ. Res.* **90**, e40 (2002).
19. Engelmayr, G. C., Jr. *et al.* Accordion-like honeycombs for tissue engineering of cardiac anisotropy. *Nat. Mater.* **7**, 1003–1010 (2008).
20. Langer, G. A. Heart: excitation-contraction coupling. *Annu. Rev. Physiol.* **35**, 55–86 (1973).
21. Noorman, M. *et al.* Cardiac cell-cell junctions in health and disease: Electrical versus mechanical coupling. *J. Mol. Cell Cardiol.* **47**, 23–31 (2009).
22. Dvir, T. *et al.* Nanowired three-dimensional cardiac patches. *Nat. Nanotechnol.* **6**, 720–725 (2011).
23. Tian, B. *et al.* Macroporous nanowire nanoelectronic scaffolds for synthetic tissues. *Nat. Mater.* **11**, 986–994 (2012).
24. You, J. O., Rafat, M., Ye, G. J. & Auguste, D. T. Nanoengineering the heart: conductive scaffolds enhance connexin 43 expression. *Nano Lett.* **11**, 3643–3648 (2011).
25. Achache, J. Keeping track of the Earth's carbon-cycle components. *Nature* **461**, 340 (2009).
26. Dai, H. Carbon nanotubes: synthesis, integration, and properties. *Acc. Chem. Res.* **35**, 1035–1044 (2002).
27. Dvir, T., Timko, B. P., Kohane, D. S. & Langer, R. Nanotechnological strategies for engineering complex tissues. *Nat. Nanotechnol.* **6**, 13–22 (2011).
28. Motta, M., Li, Y. L., Kinloch, I. & Windle, A. Mechanical properties of continuously spun fibers of carbon nanotubes. *Nano Lett.* **5**, 1529–1533 (2005).
29. Martinelli, V. *et al.* Carbon nanotubes promote growth and spontaneous electrical activity in cultured cardiac myocytes. *Nano Lett* **12**, 1831–1838 (2012).
30. Meng, X. *et al.* Novel injectable biomimetic hydrogels with carbon nanofibers and self assembled rosette nanotubes for myocardial applications. *J. Biomed. Mater. Res. A*, doi:10.1002/jbm.a.34400 (2012).
31. Shin, S. R. *et al.* Carbon-Nanotube-Embedded Hydrogel Sheets for Engineering Cardiac Constructs and Bioactuators. *ACS Nano*, doi:10.1021/nn305559j (2013).
32. Stout, D. A., Basu, B. & Webster, T. J. Poly(lactic-co-glycolic acid): carbon nanofiber composites for myocardial tissue engineering applications. *Acta Biomater.* **7**, 3101–3112 (2011).
33. Liu, D. *et al.* Solid-state, polymer-based fiber solar cells with carbon nanotube electrodes. *ACS Nano* **6**, 11027–11034 (2012).
34. Shao, S. *et al.* Osteoblast function on electrically conductive electrospun PLA/MWCNTs nanofibers. *Biomaterials* **32**, 2821–2833 (2011).
35. Zhang, W., Zhang, Z. & Zhang, Y. The application of carbon nanotubes in target drug delivery systems for cancer therapies. *Nanoscale Res. Lett.* **6**, 555 (2011).
36. Warren, C. W. Chan. *Bio-Applications of Nanoparticles Ch. 14.* (Landes Bioscience and Springer Science+Business Media, New York, 2007).
37. Sayes, C. M. *et al.* Functionalization density dependence of single-walled carbon nanotubes cytotoxicity in vitro. *Toxicol. Lett.* **161**, 135–142 (2006).
38. Agharkar, V. A., Bhushan, A., Lai, J. C. K. & Daniels, C. K. Cytotoxic Effects of Short Multi-wall Carbon Nanotubes. *Nanotech 2008 Conference Program Abstract.*
39. Yang, S. T. *et al.* Long-term accumulation and low toxicity of single-walled carbon nanotubes in intravenously exposed mice. *Toxicol. Lett.* **181**, 182–189 (2008).
40. Liu, Z. *et al.* Circulation and long-term fate of functionalized, biocompatible single-walled carbon nanotubes in mice probed by Raman spectroscopy. *Proc. Natl Acad. Sci. USA* **105**, 1410–1415 (2008).
41. Yang, S. T. *et al.* Covalently PEGylated carbon nanotubes with stealth character in vivo. *Small* **4**, 940–944 (2008).
42. Callegari, A. *et al.* Neovascularization induced by porous collagen scaffold implanted on intact and cryoinjured rat hearts. *Biomaterials* **28**, 5449–5461 (2007).
43. Piao, H. *et al.* Effects of cardiac patches engineered with bone marrow-derived mononuclear cells and PGCL scaffolds in a rat myocardial infarction model. *Biomaterials* **28**, 641–649 (2007).
44. Chi, N. H. *et al.* Cardiac repair achieved by bone marrow mesenchymal stem cells/silk fibroin/hyaluronic acid patches in a rat of myocardial infarction model. *Biomaterials* **33**, 5541–5551 (2012).
45. Christman, K. L. *et al.* Injectable fibrin scaffold improves cell transplant survival, reduces infarct expansion, and induces neovasculature formation in ischemic myocardium. *J. Am. Coll. Cardiol.* **44**, 654–660 (2004).
46. Poncelet, A. J. *et al.* Intracardiac allogeneic mesenchymal stem cell transplantation elicits neo-angiogenesis in a fully immunocompetent ischaemic swine model. *Eur. J. Cardiothorac. Surg.* **38**, 781–787 (2010).
47. Tsuji, H. *et al.* Xenografted human amniotic membrane-derived mesenchymal stem cells are immunologically tolerated and transdifferentiated into cardiomyocytes. *Circ. Res.* **106**, 1613–1623 (2010).
48. Rohr, S. Molecular crosstalk between mechanical and electrical junctions at the intercalated disc. *Circ. Res.* **101**, 637–639 (2007).
49. Bendig, G. *et al.* Integrin-linked kinase, a novel component of the cardiac mechanical stretch sensor, controls contractility in the zebrafish heart. *Genes Dev.* **20**, 2361–2372 (2006).
50. Ding, L. *et al.* Increased expression of integrin-linked kinase attenuates left ventricular remodeling and improves cardiac function after myocardial infarction. *Circulation* **120**, 764–773 (2009).
51. Hannigan, G., Troussard, A. A. & Dedhar, S. Integrin-linked kinase: a cancer therapeutic target unique among its ILK. *Nat Rev Cancer.* **5**, 51–63 (2005).
52. Magovern, J. A., Teekell-Taylor, L., Mankad, S., Dasika, U., McGregor, W., Biederman, R. W. *et al.* Effect of a flexible ventricular restraint device on cardiac remodeling after acute myocardial infarction. *ASAIO J.* **52**, 196–200 (2006).
53. Liu, Y., Sun, L., Huan, Y., Zhao, H. & Deng, J. Effects of basic fibroblast growth factor microspheres on angiogenesis in ischemic myocardium and cardiac function: analysis with dobutamine cardiovascular magnetic resonance tagging. *Eur. J. Cardiothorac. Surg.* **30**, 103–107 (2006).
54. Ou, L., Li, W., Zhang, Y., Wang, W., Liu, J., Sorg, H. *et al.* Intracardiac injection of matrigel induces stem cell recruitment and improves cardiac functions in a rat myocardial infarction model. *J. Cell Mol. Med.* **15**, 1310–1318 (2011).
55. Laflamme, M. A., Chen, K. Y., Naumova, A. V., Muskheli, V., Fugate, J. A., Dupras, S. K. *et al.* Cardiomyocytes derived from human embryonic stem cells in pro-survival factors enhance function of infarcted rat hearts. *Nat. Biotechnol.* **25**, 1015–1024 (2007).
56. Ito, H., Okamura, A., Iwakura, K., Masuyama, T., Hori, M., Takiuchi, S. *et al.* Myocardial perfusion patterns related to thrombolysis in myocardial infarction perfusion grades after coronary angioplasty in patients with acute anterior wall myocardial infarction. *Circulation.* **93**, 1993–1999 (1996).
57. Strauer, B. E., Brehm, M., Zeus, T., Köstering, M., Hernandez, A., Sorg, R. V. *et al.* Repair of infarcted myocardium by autologous intracoronary mononuclear bone marrow cell transplantation in humans. *Circulation.* **106**, 1913–1918 (2002).
58. Frangogiannis, N. G., Smith, C. W. & Entman, M. L. The inflammatory response in myocardial infarction. *Cardiovasc Res.* **53**, 31–47 (2002).

Acknowledgments

This work was supported by Key Program of National Natural Science Foundation of China (No. 31030032), National Key Basic Research and Development Program of China (No. 2011CB606206), National Natural Science Funds for Distinguished Young Scholar (No. 31025013), National High Technology Research and Development Program of China (No. 2012AA020506), National Natural Science Foundation of China (No. 31100697; 31370987).

Author contributions

C.W. (Changyong Wang), M.X. and J.Z. conceived the project and designed the experiments. J.C., X.Q., W.Z. and J.L. synthesized and characterized the materials. H.S., Y.M., C.D., Z.L., Y.Z. and Y.L. performed the experiments of construction and evaluation the engineering cardiac tissues. J.Z., X.L. and C.W. (Chunlan Wang) performed all the animal experiment *in vivo*. Y.H. and R.T. performed all the statistic analysis. C.W.

(Changyong Wang), J.Z., M.X. and Y.L. co-wrote the manuscript draft. All authors reviewed the manuscript.

Additional information

Supplementary information accompanies this paper at http://www.nature.com/scientificreports

Competing financial interests: The authors declare no competing financial interests.

How to cite this article: Zhou, J. *et al.* Engineering the heart: Evaluation of conductive nanomaterials for improving implant integration and cardiac function. *Sci. Rep.* **4**, 3733; DOI:10.1038/srep03733 (2014).